Chapter 3
Parameter Estimation of Joint Models Using Global Optimization

Robert J. Kuether and David A. Najera

Abstract Nonlinear joints and interfaces modeled with a discrete four-parameter Iwan element are defined by parameters that are often unknown a priori or require calibration to get better agreement with test data. While this constitutive model has been validated experimentally, its drawback lies in the difficulty of identifying the correct coefficients. This work proposes a parameter estimation approach using a genetic algorithm to minimize the residual between experimental and model data. Global optimization schemes have the ability to find global minima/maxima of a broad parameter space but require a very large number of function evaluations. This research focuses on decreasing the computational cost of the optimization scheme by developing a simplified model of the structure of interest and defining the objective function with amplitude dependent frequencies and damping ratios. A recently developed quasi-static modal analysis technique is used to determine these amplitude dependent properties of the model at a significantly reduced cost in comparison to solutions obtained with numerical time integration. This technique is demonstrated on a structure termed the Ministack which contains a foam-to-metal interface held together with a press fit joint.

Keywords Nonlinear joints • Parameter calibration • Global optimization • Nonlinear vibrations • Interfaces

3.1 Introduction

Common types of mechanical joints include bolted joints, compression fits, tape joints, and others. Joints maintain their strength via contact pressure and friction distributed over the contact surface, and at high enough load levels, they experience microslip or possibly full macroslip. The presence of frictional slip causes joints to have a nonlinear damping and a nonlinear stiffness, which makes their behavior difficult to model accurately. However, the ability to predict the nonlinear response of a structure with mechanical joints would greatly benefit a number of industries, including aerospace and defense where failure of critical systems can have grave consequences.

From a modeling perspective, a number of joint models have been developed to capture the phenomenological behavior of a mechanical interface, namely microslip, loss of stiffness, and nonlinear energy dissipation. One model of particular interest to this research is the four-parameter Iwan element developed by Segalman [1]. This one-dimensional element is a simplified whole joint model for use in structural dynamic simulations. Other simplified joint models include various Iwan type elements [2, 3] or the Bouc-Wen hysteresis model [4, 5]. Recently, a decoupled modal Iwan model was developed [6] to capture the nonlinear response of a mode assuming the mode shape is unchanged, and this modeling approach has been successfully applied to a realistic engineering structure [7].

One of the practical challenges involved with whole joint models, such as the four-parameter Iwan element, is the identification of the model parameters that capture the characteristic behavior of the interface. The four parameters of a modal Iwan model can be estimated by applying a modal filter to measured transient ring-down data and taking the Hilbert transform to estimate the nonlinear damping and frequency [6, 7]. A whole joint model can also be calibrated to test data

Sandia National Laboratories is a multi-mission laboratory managed and operated by Sandia Corporation, a wholly owned subsidiary of Lockheed Martin Corporations, for the U.S. Department of Energy's National Nuclear Security Administration under Contract DE-AC04-94AL85000

R.J. Kuether (✉)
Sandia National Laboratories, Albuquerque, NM 87185, USA
e-mail: rjkueth@sandia.gov

D.A. Najera
ATA Engineering, Inc., San Diego, CA 92128, USA

M.S. Allen et al. (eds.), *Dynamics of Coupled Structures, Volume 4*, Conference Proceedings of the Society for Experimental Mechanics Series, DOI 10.1007/978-3-319-54930-9_3

by using optimization techniques to minimize the residual between the data predicted by the numerical model and the measured data. Examples of this include the work by Charalampakis et al. [8, 9] who developed an identification method to determine the parameters of a Bouc-Wen hysteretic model using different global optimization schemes. Wang et al. [10] presented a joint model updating scheme using analytical mode decomposition to extract the instantaneous characteristics of the measured and numerically integrated response. These cost function metrics are used with a simulated annealing global optimization method to identify the optimal joint parameters.

The research presented here proposes to model the mechanical interface of a structural dynamic model with a four-parameter Iwan element and use the genetic algorithm implemented in [11] to calibrate the joint parameters. The genetic algorithm is a global optimization scheme that explores a broad parameter space and does not require an initial guess. Using global optimization over gradient based schemes is more computationally expensive since it demands more evaluations of the objective function, but has the advantage of finding global optimum. Because of this, quasi-static modal analysis [12] is used to estimate the amplitude dependent frequency and damping of the nonlinear mode of interest. Since this approach computes the instantaneous properties of the nonlinear model with a static solution, the proposed calibration scheme significantly reduces the computational effort needed to evaluate the objective function.

The sections of the paper are as follows. Section 3.2 briefly reviews the four-parameter Iwan formulation along with the optimization scheme developed to calibrate the parameters. Section 3.3 demonstrates the methodology on a simplified model of the "Ministack" hardware, which consists of a press fit joint of a metal slug within a foam encapsulant. The parameters of the nonlinear model are calibrated to experimental swept sine data of the real hardware. Section 3.4 discusses the conclusion.

3.2 Modeling and Calibration

3.2.1 Whole Joint Models

In structural dynamics, a whole joint modeling approach condenses a mechanical interface down to a discrete nodal location at which a pointwise constitutive model is used to describe the interface forces. This joint modeling approach reduces the time and length scales of the joint model for structural dynamics simulations requiring many time steps over a large period. Detailed interface models with Coulomb friction and node-to-node contact require detailed meshes not amenable to structural dynamics. The whole joint modeling philosophy relies on the assumption that the local kinematics at the interface do not significantly contribute to the response, since multi-point constraints (MPCs) are often used to tie a set of nodes on the contact surface down to a single point. Figure 3.1 shows an example of how MPCs tie to a surface to a single node to resemble the kinematics of three bolted joints in a beam.

One of the constitutive equations used within the whole joint model is the four-parameter Iwan element that was originally derived for lap-type joints [1]; the theory is briefly reviewed here. This constitutive model captures the microslip behavior

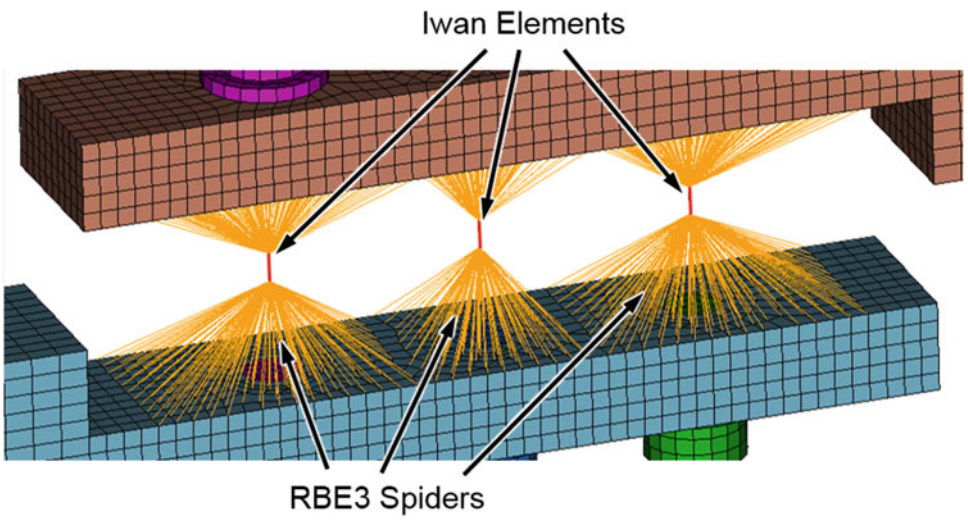

Fig. 3.1 Example of a whole joint model of three bolts in a lap-joint [13]

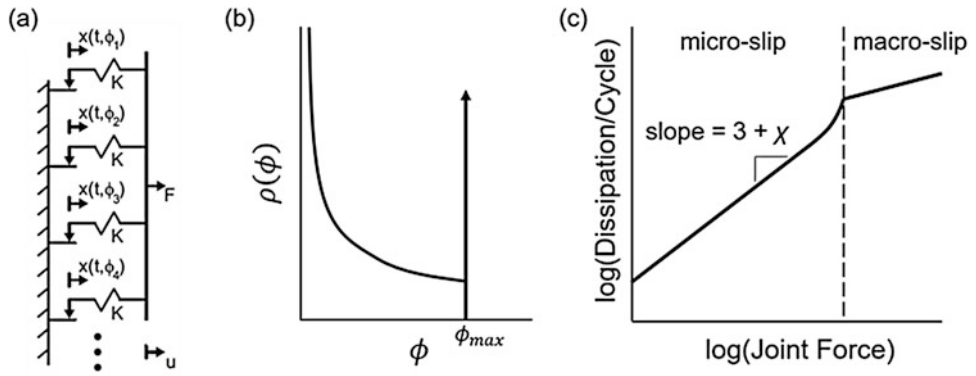

Fig. 3.2 Schematic of the (**a**) parallel-series Iwan element, (**b**) power-law population distribution, and (**c**) power-law energy dissipation versus force (Image from Gross et al. [13])

and nonlinear dependence of damping as the amplitude of the response increases, as well as a loss of stiffness at larger amplitudes. The force of a parallel-series Iwan model is written as,

$$F(t) = \int_0^\infty \rho(\varphi)\left[u(t) - x(t,\varphi)\right] d\varphi \tag{3.1}$$

with the stick/slip condition definitions,

$$\dot{x}(t,\varphi) = \begin{cases} \dot{u} & \text{if } \|u - x(t,\varphi)\| = \varphi \quad \text{and} \quad \dot{u}\left[u - x(t,\varphi)\right] > 0 \\ 0 & \text{otherwise} \end{cases} \tag{3.2}$$

The dimensionless values, $x(t,\varphi)$, are the displacement of the Jenkins elements with a slip displacement φ, $\rho(\varphi)$ is the population density of Jenkins elements of strength φ, and $u(t)$ and $F(t)$ are the joint displacement and applied force, respectively. The schematic in Fig. 3.2. shows the Iwan element as a set of Jenkins elements along with the population density and energy dissipation versus joint force.

Assuming a power-law population distribution that is terminated at a finite displacement,

$$\rho(\varphi) = R\varphi^{\chi}\left[H(\varphi) - H(\varphi - \varphi_{\max})\right] + S\delta(\varphi - \varphi_{\max}) \tag{3.3}$$

Substituting this equation into Eq. (3.1), the force-displacement relationship becomes,

$$F(t) = \int_0^{\varphi_{\max}} \left[u(t) - x(t,\varphi)\right] R\varphi^{\chi} d\varphi + S\left[u(t) - x(t,\varphi_{\max})\right] \tag{3.4}$$

where the parameters of the Iwan element are defined as,

$$R = \left(\frac{F_s(1+\chi)}{\varphi_{\max}^{\chi+2}\left(\beta + \left(\frac{\chi+1}{\chi+2}\right)\right)}\right) \tag{3.5}$$

$$S = \left(\frac{F_s}{\varphi_{\max}}\right)\left(\frac{\beta}{\beta + \left(\frac{\chi+1}{\chi+2}\right)}\right) \tag{3.6}$$

$$\varphi_{\max} = \left(\frac{F_s(1+\beta)}{K_T\left(\beta + \left(\frac{\chi+1}{\chi+2}\right)\right)}\right) \tag{3.7}$$

The Iwan element in Eq. (3.4) in conjunction with Eqs. (3.5), (3.6), and (3.7) is completely defined by the following parameters: F_s (slip force), K_T (joint stiffness when no slip occurs), χ (exponent describing slope of force-dissipation curve), and β (shape parameter of the force-dissipation curve near transition to macroslip). As discussed in [1], these parameters are preferred since they are "measureable" quantities. The slip force can be estimated from static calculations with an assumed Coulomb friction coefficient, while the low amplitude stiffness can be estimated by performing vibration tests at low excitation levels. Determining the values for χ and β is a bit more challenging and requires specific harmonically loaded experiments to calibrate.

3.2.2 Objective Function

Calibrating Iwan parameters (F_s, K_T, χ, β) can be difficult when the specific set of experiments are unavailable or too costly to run. Furthermore, finite element models with many joints, such as the one shown above in Fig. 3.1, could potentially have joint models with different parameters requiring calibration data. This section proposes a joint model calibration scheme that uses measured vibration data to identify the optimal parameters. First, a least squares objective function is defined in order to minimize the difference between the measured and predicted output,

$$\Gamma = \frac{1}{N}\sum_{i=1}^{N}\left(\frac{y-\tilde{y}\left(\mathbf{p}\right)}{y}\right)^2 \tag{3.8}$$

The measured output, y, is obtained from test data and the predicted output, $\tilde{y}$, is the solution to the model for a given set of parameters, $\mathbf{p}$. A global optimization scheme makes numerous evaluations of this objective function so it is important to make the model simulations as inexpensive as possible.

Calibration algorithms for linear finite element models rely on invariant modal properties to define the residuals in the objective function in Eq. (3.8). Since the Iwan elements introduce nonlinear behavior, a new metric is sought to capture the important characteristics of the system. Recently Allen et al. [12] developed a quasi-static modal analysis technique that estimates the amplitude dependent natural frequency and damping ratio of a finite element model with Iwan elements. The approach works by applying a quasi-static force in the shape of the linearized mode and computing the nonlinear quasi-static response. From this force-displacement relationship, the secant of the loading curve provides an estimate of the amplitude dependent frequency, while the full hysteresis curve obtained using Masing's rules is used to estimate the effective damping for the given response amplitude. These two effective modal properties are used to define the objective function for the genetic algorithm described in the next subsection,

$$\Gamma_{\mathrm{GA}} = \frac{\eta}{N}\sum_{i=1}^{N}\left(\frac{\omega_n\left(a_i\right)-\tilde{\omega}_n\left(a_i,\mathbf{p}\right)}{\omega_n\left(a_i\right)}\right)^2 + \frac{(1-\eta)}{N}\sum_{i=1}^{N}\left(\frac{\zeta\left(a_i\right)-\left(\tilde{\zeta}_{Iwan}\left(a_i,\mathbf{p}\right)+\tilde{\zeta}_{viscous}\right)}{\zeta\left(a_i\right)}\right)^2 \tag{3.9}$$

Here the amplitude dependent natural frequencies, $\tilde{\omega}_n\left(a_i,\mathbf{p}\right)$, and damping ratios $\tilde{\zeta}_{Iwan}\left(a_i,\mathbf{p}\right)$, are computed from the quasi-static approach for a set of model parameters, $\mathbf{p}$. The experimental data, $\omega_n(a_i)$ and $\zeta(a_i)$, can been estimated with either swept sine or transient ring-down tests as done in [14]. The scalar η is the weight coefficient used to give more or less importance to the frequencies or the damping ratios; a value of $\eta = 0.5$ gives equal weight to both properties.

Figure 3.3 shows a comparison of the amplitude dependent frequency and damping from simulated swept sine tests and the quasi-static modal analysis. The simplified model introduced later in Sect. 3.3.2 was used to generate this numerical data. Comparisons between the quasi-static modal analysis and transient ring-down data have been reported in [12]. The agreement between the frequency and damping estimates from both techniques suggests that the quasi-static approach can be used to simulate the model and obtain the same meaningful information as would be obtained from sine sweep data. Computing swept sine responses from a model would add significantly more computational effort per function evaluation of Eq. (3.8) and slow down the global optimization algorithm needed to explore the broad parameter space. Simulating the quasi-static analysis demands much less computational effort and hence is more desirable for use in the optimization algorithm.

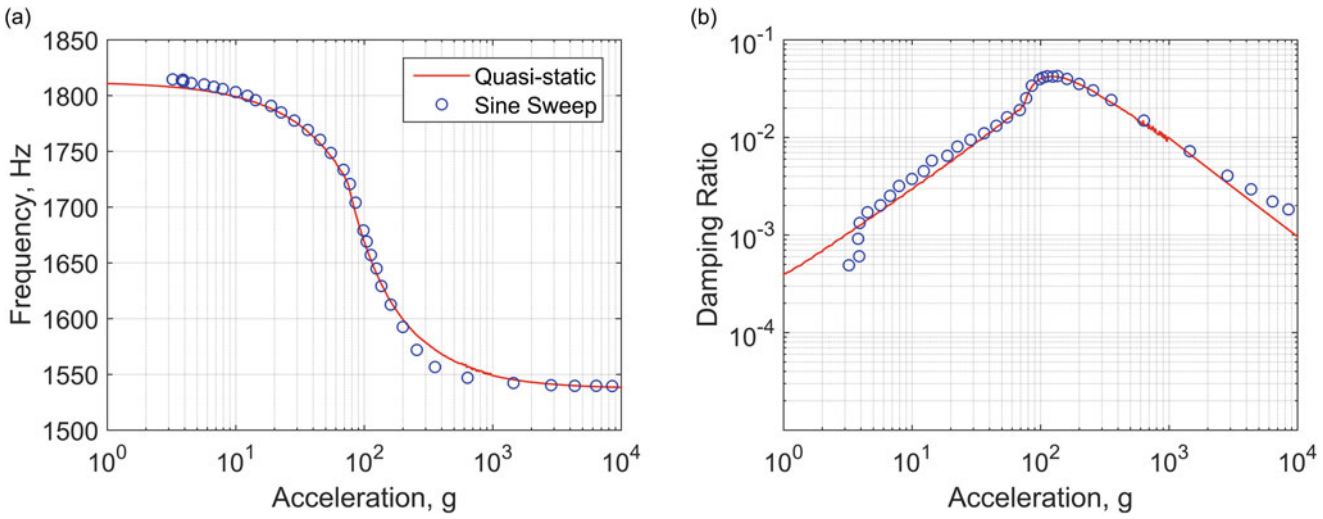

Fig. 3.3 Amplitude dependent (**a**) frequencies and (**b**) damping ratios for a simplified two degree-of-freedom model

3.2.3 Genetic Algorithm

A genetic algorithm (GA) is used to calibrate the Iwan parameters since it is a global optimization method that balances broad exploration of the parameter space with computational efficiency. It is usually better suited than gradient-based algorithms when multiple optima exist, but is more computationally expensive due to the number of function evaluations. GA is part of the family of evolutionary algorithms and relies on operators inspired by biological evolution. A random set of candidate solutions known as "individuals" are generated, forming a "population". At each generation, each individual has a set probability of "mutating", which is the main mechanism used for exploration of new solutions. In the case of joint model calibration, a Gaussian mutation operation is used. Individuals are also able to "mate" thus generating new solutions based on the combination of the fittest individuals in a given generation, where fitness is the value of the objective function. After mutation and mating, there is a selection process during which only the fittest individuals make it to the next generation. This process is repeated until convergence is reached and variance in the population is low. The GA algorithm used to calibrate the joint models is implemented in Python using the DEAP package [11].

3.3 Results

3.3.1 Experimental Hardware and Data

Test data was collected from a system termed the "Ministack" which consists of a solid aluminum 6061-T6 mass that fits into two 20 pounds per cubic foot closed cell PMDI foam cups. This subassembly is then inserted into an aluminum can, and a steel disk covering the top of the foam holds a nominal 700 lbf preload that is held in place with a threaded steel ring. The base plate of the can is then bolted to the shaker table for vibration testing. A schematic of the setup is shown below in Fig. 3.4. For reference, the solid aluminum mass (i.e. slug) is 4 inches high with a diameter of 3 inches. The foam cups each have an average inner depth of 2 inches, with an average inner diameter of 2.99 inches. As a result, the slug nominally fits tightly within the foam casing allowing for the preload to go through both the foam cups and the aluminum slug. In axial base excitation, the axial mode of the slug is expected to exercise the large foam-to-metal interface between the slug and foam cups and be the main source of nonlinear behavior.

A uniaxial control accelerometer was placed in a recess at the bottom of the base plate, and a triaxial accelerometer was attached to a cavity located on top of the slug (as seen in the left of Fig. 3.4). A series of sine sweep tests were carried out at various excitation levels to observe the nonlinear behavior near the resonance of the dominant axial mode. The test series is given below in Table 3.1. Prior to testing, the Ministack hardware was assembled by applying a preload via a press until the reading on the load cell was approximately the nominal value of 700 lbf. The retaining ring was tightened to maintain the preload, the press was released, and Ministack was then bolted to the shaker. The base plate of the can was accelerated

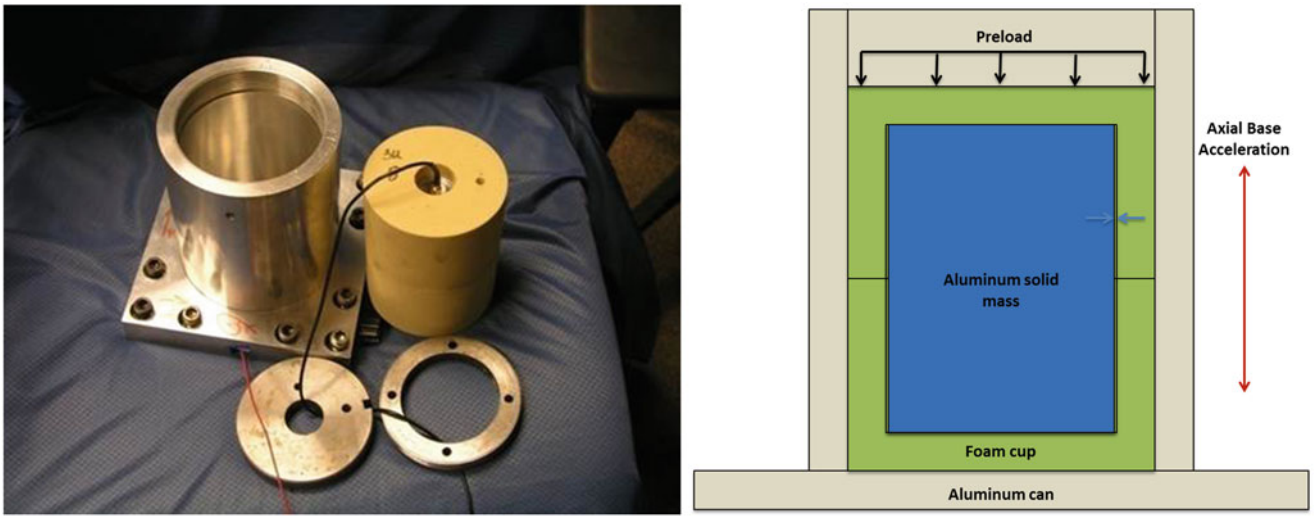

Fig. 3.4 Ministack hardware

Table 3.1 Sine Sweep test series for Ministack assembly

Test ID	Sweep series amplitudes
1	1 g up, 1 g down, 1 g up, 1 g down, 1 g up, 1 g down
2	2 g up, 2 g down
3	5 g up, 5 g down
4	10 g up, 10 g down

with a swept sine input between 700 and 2500 Hz at a linear rate. The first test was a sweep at 1 g amplitude from 700 to 2500 Hz (up), followed by a 1 g sweep from 2500 to 700 Hz (down). This was repeated two more times at a 1 g load level to allow the slug to "settle" within the foam cups. Following the 1 g sweeps, the Ministack was excited from 700 to 2500 Hz at a 2 g level, and then back down from 2500 to 700 Hz. The same upward and downward tests were then run at 5 g and 10 g levels, and the hardware was disassembled and reassembled, carefully noting the alignment as not to change the orientation of the components. The same tests were repeated for the reassembled hardware in order to observe any variability between two assembly processes.

The axial slug acceleration was processed using the short-time Fourier transform to estimate the envelope of the signal in the frequency domain. These results are shown below in Fig. 3.5 for all the downward sweeps (the 1 g sweep was the last of the three in the test series). There seemed to be some slight directional dependence of the sweep frequency (not shown here) but for the most part the upward and downward sweeps showed very similar responses. The envelopes of the response show that as the amplitude of the base acceleration increased, the resonant frequency decreased. This is consistent with the nonlinear behavior of microslip in mechanical joints. The resonant frequencies were determined from the swept sine test data by identifying the frequency at which the input and response were 90 degrees out-of-phase from one another. The effective damping was estimated via the half power bandwidth rule. The plots in Fig. 3.6 show the effective frequencies and damping ratios from the sine sweep data in Fig. 3.5 which served as the reference data of the objective function in Eq. (3.9) with which the model was calibrated.

3.3.2 Optimal Model Parameters

A simplified two degree-of-freedom system of equations was generated in order to model the dynamics of the Ministack hardware in Fig. 3.4. The schematic in Fig. 3.7 shows the discrete model of a slug mass, m_{slug}, connected to the can and the shaker mass, m_{can}, through parallel linear spring and Iwan elements. The mass of the aluminum slug was measured to be 2.65 lbf while the mass of the can plus shaker were assumed to be 386,000 lbf. The latter value was chosen in order to numerically apply a base acceleration as an external force.

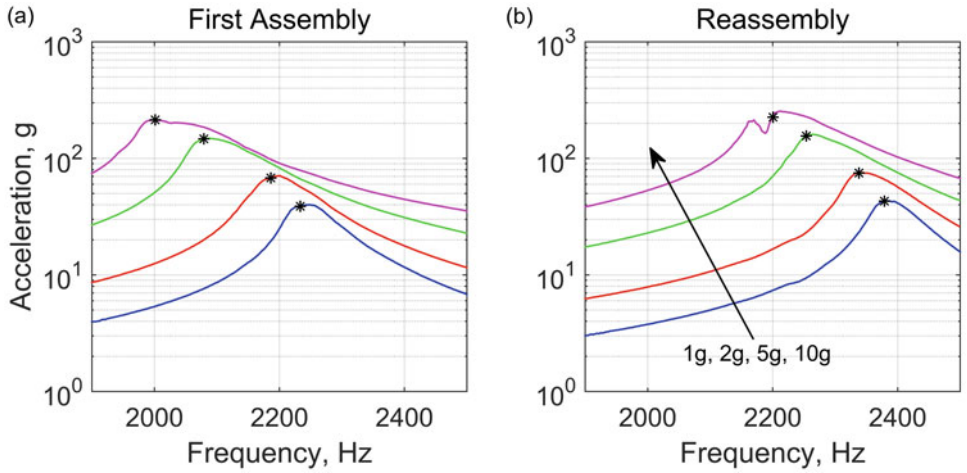

Fig. 3.5 Swept sine response envelopes for (**a**) initial assembly and (**b**) disassembly + reassembly

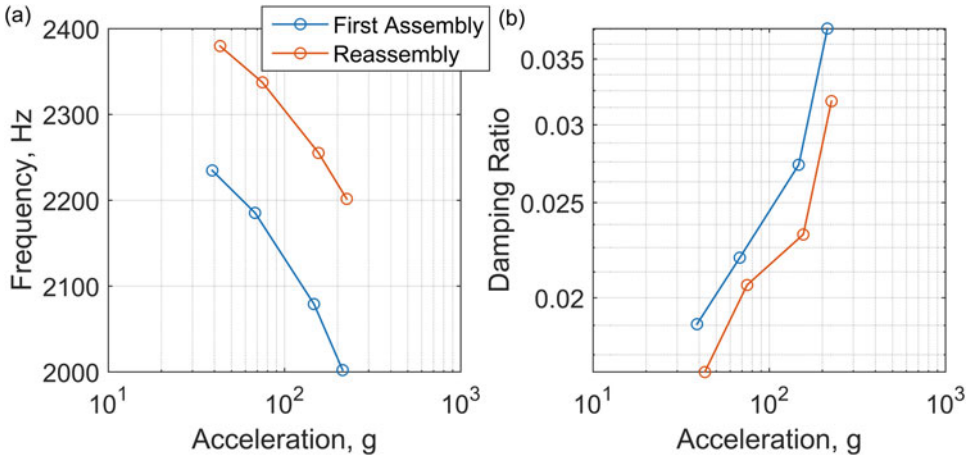

Fig. 3.6 Amplitude dependent (**a**) resonant frequencies and (**b**) damping ratios estimated from swept sine tests for initial assembly and disassembly + reassembly

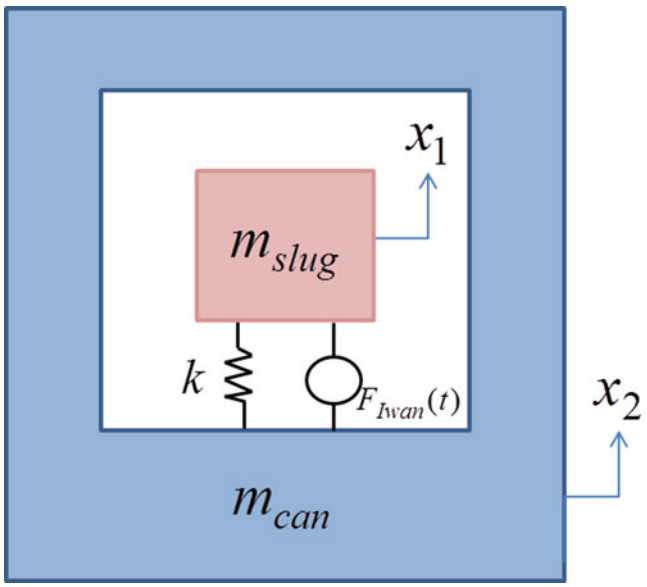

Fig. 3.7 Schematic of simplified Ministack model

Table 3.2 Optimal model parameters.

	Iwan parameters				Linear parameters	
	$F_s(lbf)$	$K_T(lbf/in)$	χ	β	$k(lbf/in)$	$\zeta_{viscous}$
First assembly	313	1.02×10^6	−0.65	0.004	6.12×10^5	0.0015
Reassembly	274	0.90×10^6	−0.61	0.025	8.56×10^5	0.0017

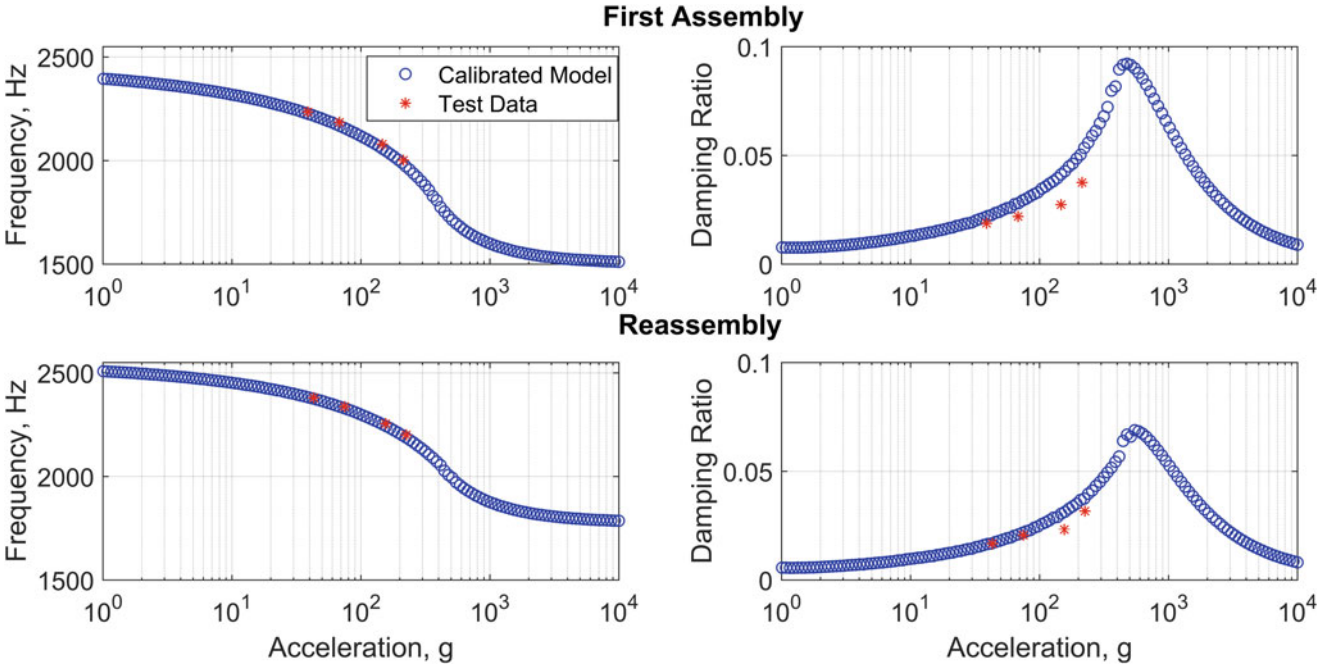

Fig. 3.8 Comparison of amplitude dependent frequencies and damping ratios from experiment and calibrated model for the (*top row*) initial assembly and (*bottom row*) disassembly + reassembly

The GA optimization and quasi-static modal analysis were applied to the simplified two degree-of-freedom model to estimate the four Iwan parameters (F_s, K_T, χ, β). In addition, the linear spring stiffness (k) and viscous damping ratio ($\zeta_{viscous}$) were also treated as unknowns. Due to the uncertainty of the damping ratios extracted from the test data, the weight coefficient, η, was set to 0.85 to more heavily weight the frequencies in Eq. (3.9). The resulting optimal model parameters found from the optimization routine are presented in Table 3.2 forthe initial assembly and disassembly + reassembly configurations. The linear viscous damping was effectively the same between the two configurations, but was lower than expected since the foam cups should introduce damping levels higher than ∼0.1%. The linear spring stiffness shifted up when the system was reassembled and could be explained by the time dependent behavior of the foam under an uncertain level of preload. The Iwan parameters were in relatively good agreement between the two assemblies, with the exception of β. The slight change in slip force, F_s, and joint stiffness, K_T, could be explained by the change in load path between the can, foam and slug, as well as the relaxation of stresses within the foam. The slope of the energy dissipation curve, χ, agrees well between the two models suggesting that the power-law energy dissipation behavior is consistent for the press fit joint.

A comparison of the response obtained with the calibrated model using the quasi-static method and test data for initial assembly and disassembly + reassembly is shown in Fig. 3.8. The optimization algorithm was able to get the simplified model to predict frequencies that agreed very well with the test data and reasonably well for the damping ratios. The model was computed over a broad range of response amplitudes to show where the test data lies within the range of nonlinear stiffness and damping.

Figures 3.9 and 3.10 illustrate the design space explored by the GA. The scatter plots show the interactions between different model parameters and how they were explored. The plot in the last row and column show the value of the objective function as a function of the different parameters as they were explored. Plots along the diagonal are density plots showing

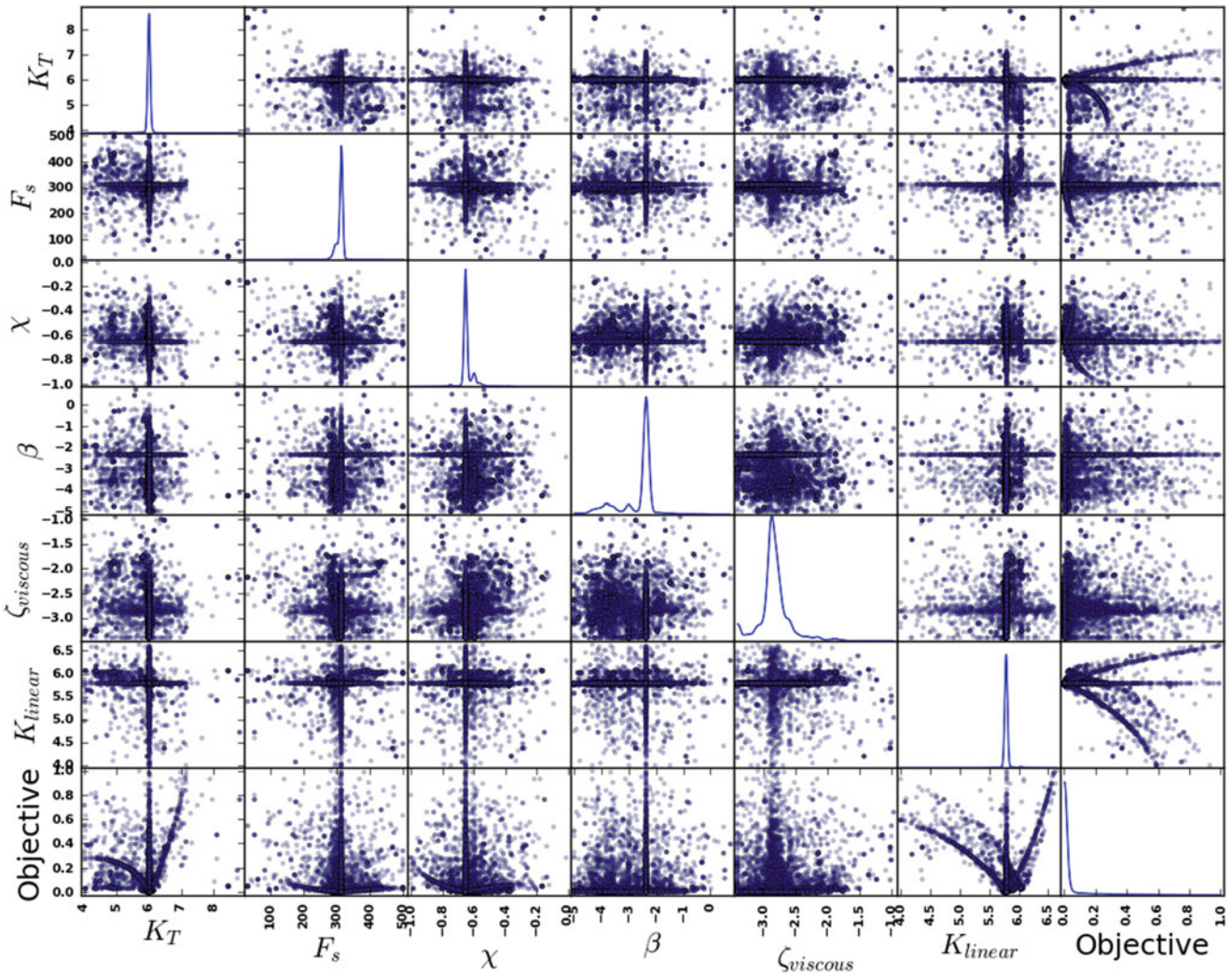

Fig. 3.9 Scatter plot matrix of GA exploration for initial assembly model parameters and objective function values

where the algorithm spent most of the time. The peaks of the density plots correlate with the optimal parameters ultimately chosen. These plots show that there was broad exploration of the parameter space and that a clear minimum emerged from the objective function.

3.3.3 Validation with Sine Sweeps

A final validation step was done to check how well the simplified, calibrated model could predict the experimental swept sine response. During testing, the axial base acceleration was measured with a control accelerometer and used as the input into the discrete model. Figure 3.11 shows the comparison between the experimentally measured response envelopes (solid lines) and the predicted envelopes (dashed lines) for the 1, 2, 5 and 10 g levels. The model under predicts the response amplitude for each input, however the resonant peaks appear to align with one another. It was observed in the control signal that the accelerometer had significant amplification as the shaker swept through the resonance. The input signal could have some significant coupling between the shaker and the Ministack that would not be captured by the model (the can and shaker were modeled as a rigid mass). Development of a higher fidelity model may better capture the flexibility of the Ministack and improve the ability of the model to predict the swept sine response.

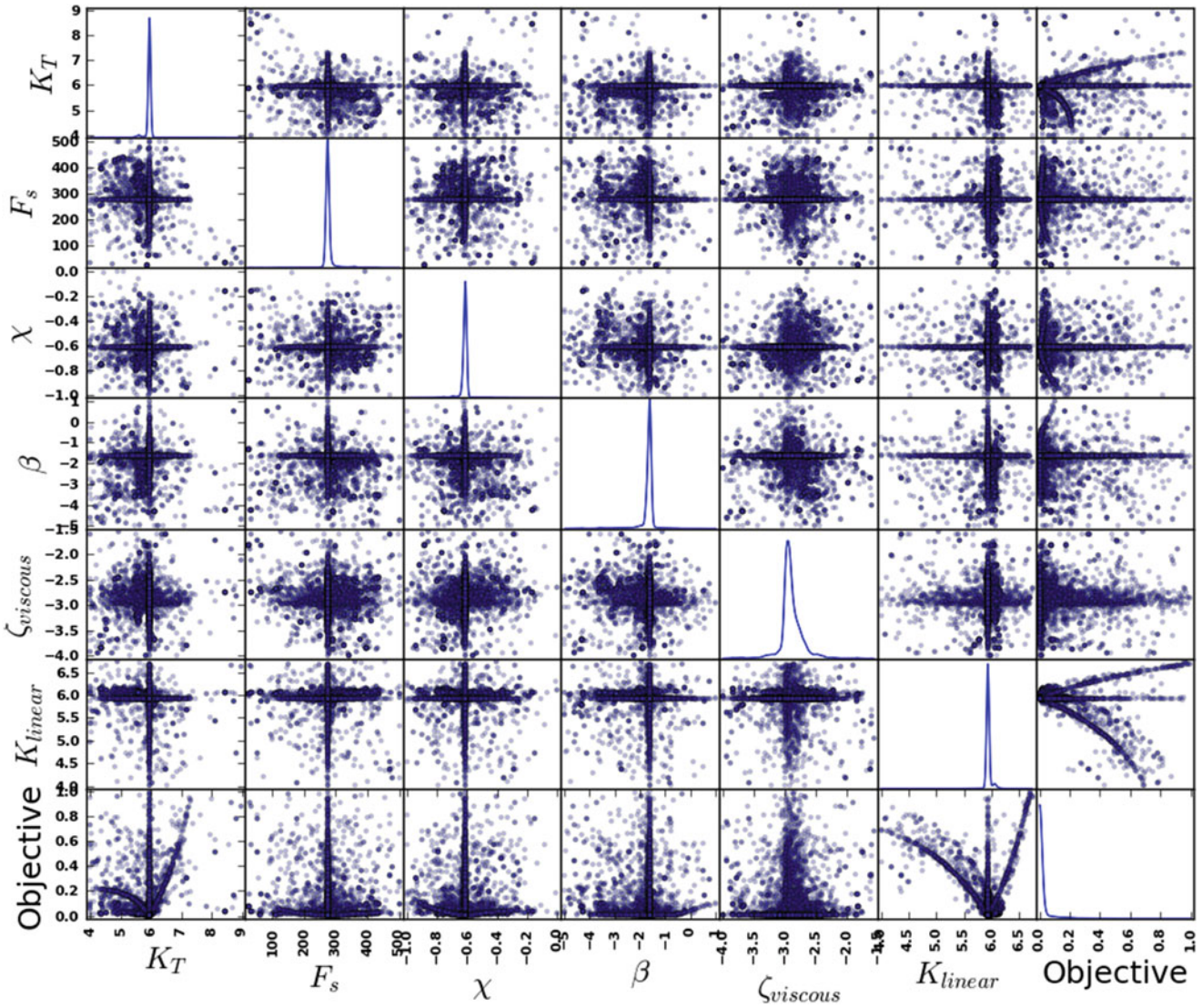

Fig. 3.10 Scatter plot matrix of GA exploration for disassembly + reassembly model parameters and objective function values

3.4 Conclusion

This research developed a joint model calibration scheme using global optimization and quasi-static modal analysis. A genetic algorithm was used due to its ability to search a broad parameter space and find global optimum. Since this approach typically requires an increased number of function evaluations, the quasi-static modal analysis was used to efficiently compute the amplitude dependent frequencies and damping ratios of the nonlinear model. These dynamic characteristics defined the least squares objective function used to evaluate the fitness of the parameters of the joint model. This method was demonstrated using the Ministack hardware, which consisted of a press fit joint of a metal slug within a foam encapsulant. A simplified two degree-of-freedom model was created to capture the dynamics of the fundamental axial vibration mode and the foam-to-metal interface was modeled with a four-parameter Iwan element. Experimental swept sine data taken from the Ministack hardware was used to determine the amplitude dependent frequencies and damping, and the model was calibrated to match this data. An optimal set of Iwan parameters were identified for two different assembly steps, and showed that the interface properties were only slightly affected by the reassembly. The validation step of the model unfortunately showed that the model was not in perfect agreement with the test data, and that the responses were under predicted. Development of a higher fidelity model could improve the ability to capture the experimental response.

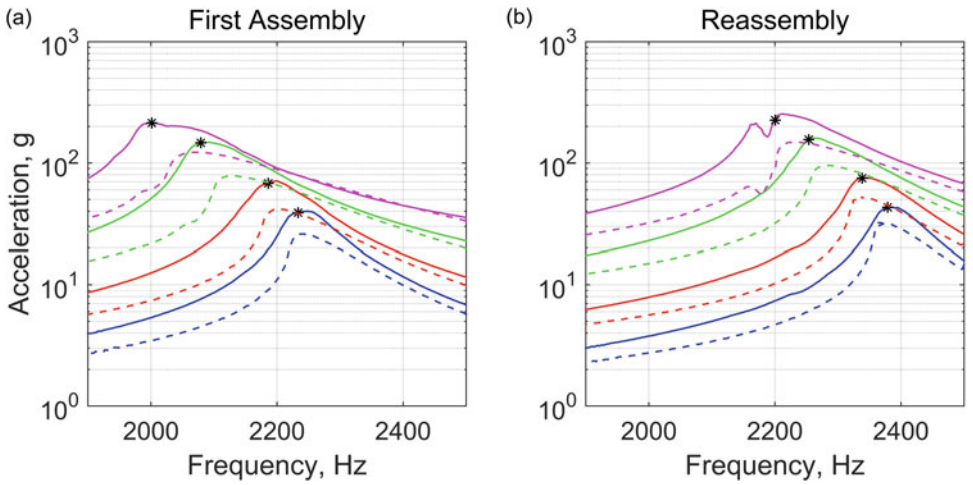

Fig. 3.11 Swept sine response envelopes for (**a**) initial assembly and (**b**) disassembly + reassembly; (*solid lines*) test data (*dashed lines*) calibrated model

Acknowledgements The authors would like to thank Matt Allen and Bob Lacayo from the University of Wisconsin-Madison for sharing their codes to run the quasi-static modal analysis on discrete models. The authors would also like to thank Laura Jacobs and John Hofer for their efforts in measuring the experimental data on the Ministack hardware. This work was funded by Sandia National Laboratories. Sandia National Laboratories is a multi-mission laboratory managed and operated by Sandia Corporation, a wholly owned subsidiary of Lockheed Martin Corporation, for the U.S. Department of Energy's National Nuclear Security Administration under contract DE-AC04-94AL85000.

References

1. Segalman, D.J.: A four-parameter Iwan model for lap-type joints. J. Appl. Mech. **72**, 752–760 (2005)
2. Li, Y., Hao, Z.: A six-parameter Iwan model and its application. Mech. Syst. Signal Process. **68–69**, 354–365 (2016)
3. Mignolet, M.P., Song, P., Wang, X.Q.: A stochastic Iwan-type model for joint behavior variability modeling. J. Sound Vib. **349**, 289–298 (2015)
4. Bouc, R.: Forced vibration of mechanical systems with hysteresis. Presented at the Fourth Conference on Non-linear Oscillation, Prague, Czechoslovakia, 1967
5. Wen, Y.-K.: Method for random vibration of hysteretic systems. J .Eng. Mech. Div. **102**, 249–263 (1976)
6. Deaner, B.J., Allen, M.S., Starr, M.J., Segalman, D.J., Sumali, H.: Application of viscous and Iwan modal damping models to experimental measurements from bolted structures. J. Vib. Acoust. **137**, 021012 (2015)
7. Roettgen, D.R., Allen, M.S.: Nonlinear characterization of a bolted, industrial structure using a modal framework. Mech. Syst. Signal Process. 84B, 152–170 (2017)
8. Charalampakis, A.E., Dimou, C.K.: Identification of Bouc–Wen hysteretic systems using particle swarm optimization. Comput. Struct. **88**, 1197–1205 (2010)
9. Charalampakis, A.E., Koumousis, V.K.: Identification of Bouc–Wen hysteretic systems by a hybrid evolutionary algorithm. J. Sound Vib. **314**, 571–585 (2008)
10. Wang, Z.-C., Xin, Y., Ren, W.-X.: Nonlinear structural joint model updating based on instantaneous characteristics of dynamic responses. Mech. Syst. Signal Process. **76–77**, 476–496 (2016)
11. Fortin, F.-A., Rainville, F.-M.D., Gardner, M.-A., Parizeau, M., Gagné, C.: DEAP: evolutionary algorithms made easy. J. Mach. Learn. Res. **13**, 2171–2175 (2012)
12. Allen, M.S., Lacayo, R.M., Brake, M.R.W.: Quasi-static modal analysis based on implicit condensation for structures with nonlinear joints. Presented at the ISMA2016 – International Conference on Noise and Vibration Engineering, Leuven, Belgium, 2016
13. Gross, J., Armand, J., Lacayo, R.M., Reuß, P., Salles, L., Schwingshackl, C.W., et al.: A numerical round robin for the prediction of the dynamics of jointed structures. Presented at the 34th International Modal Analysis Conference (IMAC XXXIV), Orlando, Florida, 2016.
14. Sumali, H., Kellogg, R.A.: Calculating damping from ring-down using Hilbert transform and curve fitting. In 4th International Operational Modal Analysis Conference (IOMAC), Istanbul, Turkey, May, 2011, pp. 9–11